Int. J. Mach. Tool Des. Res. Vol. 26, No. 1, pp. 1–14, 1986.
Printed in Great Britain

0020–7357/86 $3.00+.00
Pergamon Press Ltd.

J19

ESTIMATION OF RAKE TEMPERATURES IN FREE OBLIQUE CUTTING

P. K. VENUVINOD* and W. S. LAU*

(*Received* 27 *July* 1984; *received for publication* 5 *February* 1985)

Abstract—A model for analysing temperatures in free oblique cutting with sharp cutting tools is developed by utilising a recent solution for temperature distributions on a rectangular heat source moving obliquely on a semi-infinite conducting medium. The source obliquities introduced at the shear and rake planes by the tool obliquity are identified and a procedure is developed to compute the temperature distributions and heat partition coefficients at the shear and rake planes. For mild steel cut by a H.S.S. tool, the mean tool–chip interface temperature estimated by the new model is in close agreement with that measured by the tool–work thermocouple method. It is noted that the introduction of tool obliquity results in temperature and heat partition coefficient distributions which are essentially similar to those obtained in orthogonal cutting. The mean tool–chip interface temperature is found to decrease with increasing tool obliquity.

NOMENCLATURE

b	wall thickness of tubular workpiece
c_s	volume specific heat of work material at shear plane
C_n	tool–chip contact length
f_1, $\bar{f}_1$	functions defined in the text
f_c, f_v, f_r	reduced cutting forces (forces directly related to chip formation) in the directions of F_c, F_v and F_r respectively
F	tangential force component at the tool–chip interface
F_c	cutting force component in the direction of cutting speed
F_v	cutting force component normal to the machined surface
F_r	cutting force component perpendicular to both F_c and F_v
i	index of source element at tool–chip interface
i'	index of sub-area at tool rake surface
$I(i', i)$	chip side influence coefficient relating heat source i to sub-area i'
J	mechanical equivalent of heat
$J(i', i)$	tool side influence coefficient relating heat source i to sub-area i'
$J'(i', i)$, $J''(i', i)$	parameters defined in the text
k_c, k_t	thermal conductivities of the chip and tool materials respectively
k_m	thermal conductivity of a conducting medium
k_s	thermal conductivity of work material at shear plane
K_s, K_r	constants
l'	half length of a rectangular heat source
L, L_c	parameters defined in the text
m	number of heat source elements at tool–chip interface
m'	half width of a rectangular heat source
m''	number of heat source elements within the sticking zone at tool–chip interface
M, M_c	parameters defined in the text
q^*	rate of heat flux per unit area entering a semi-infinite conducting medium from a rectangular heat source moving on it
$q_{c,i}$	mean rate of heat flux per unit area entering the chip at source element i
q_r	mean rate of heat generation per unit area at tool–chip interface
$q_{r,i}$	mean rate of heat flux per unit area generated at source element i
q_s	mean rate of heat flux generation per unit area at shear plane
$q_{t,i}$	mean rate of heat flux per unit area entering the tool at source element i
$R_{r,i}$	heat partition coefficient (fraction entering the tool) at source element i
$\bar{R}_r$	mean heat partition coefficient (fraction entering the tool) at tool–chip interface
R_s	mean heat partition coefficient (fraction entering the chip) at shear plane
S	shear force on the shear plane
t	time
t_1	uncut chip thickness
t_2	chip thickness

* Department of Production and Industrial Engineering, Hong Kong Polytechnic, Hung Hom, Kowloon, Hong Kong.

u	a parameter defined in the Appendix
V	cutting speed; velocity of a rectangular heat source relative to a semi-infinite conducting medium
V_c	chip speed
V_s	velocity of shear at the shear plane
w	a parameter defined in the text
W	length of cutting edge in contact with workpiece
x	coordinate of a point on a semi-infinite conducting medium
Δx	half width of sub-areas at tool–chip interface
X, $X_{i'i}$, X_t	parameters defined in the text
y	coordinate of a point on a semi-infinite conducting medium
Y, $Y_{i'i}$, Y_t	parameters defined in the text
α_m	thermal diffusivity of a conducting medium
α_c, α_s	thermal diffusivities of the chip material at the tool–chip interface and the shear plane respectively
α_n	normal rake angle
ϵ', ϵ_r	indices of V in power laws relating $\bar{\theta}_s$ and $\bar{\theta}_r$ respectively to V
η_c	chip flow angle
η_s	deviation of V_s from the normal to the cutting edge in the shear plane
η', η_r	indices of t_1 in power laws relating $\bar{\theta}_s$ and $\bar{\theta}_r$ respectively to t_1
θ_0	ambient temperature
$\theta_{c,\,i'}$	temperature at the centre of sub-area i' calculated from the chip side
θ_m	tool–work thermocouple temperature
$\theta_{r,\,i'}$	temperature at the centre of sub-area i' at tool–chip interface
θ_r	rake temperature
$\bar{\theta}_s$	mean temperature at shear plane
$\theta_{t,\,i'}$	temperature at centre of sub-area i' calculated from the tool side
$\Delta\bar{\theta}$	mean temperature rise over a rectangular heat source moving on a semi-infinite conducting medium
$\Delta\theta\ (x,y)$	temperature rise at point (x, y)
$\Delta\bar{\theta}_{s,\,c}$	mean temperature rise at shear plane calculated from the chip side
$\Delta\bar{\theta}_{s,\,w}$	mean temperature rise at the shear plane calculated from the workpiece side
λ	tool obliquity
ϕ_n	normal shear angle
Φ	obliquity of motion of a rectangular heat source

INTRODUCTION

ALTHOUGH the majority of practical cutting operations are oblique, the analysis of oblique cutting has received far less attention than has the analysis of the particular case of zero obliquity i.e. orthogonal cutting. Further, most of the literature on oblique cutting refers to the mechanics of chip formation while, in contrast, little exists on cutting temperatures and tool wear analyses. In the present work attention will be concentrated on a method to predict cutting temperatures as a prerequisite to tool wear prediction.

Most of the analyses of cutting temperatures in orthogonal cutting, for example [1–4], make use of classical theories of conduction heat transfer employing rectangular moving heat sources with uniformly distributed heat fluxes. For instance, in orthogonal cutting, the heat source at the tool–chip interface may be approximated by a rectangular source with sides W and C_n where W is the length of cutting edge in engagement and C_n is the natural tool–chip contact length. From the point of view of the chip, in orthogonal cutting, this source is moving in a direction perpendicular to one of its sides, namely W, at a speed equal to chip speed V_c. The basic equations governing heat transfer across such "orthogonally moving" rectangular heat sources are readily available [5, 6].

The above idealisation however is not applicable to oblique cutting where the chip velocity vector V_c is inclined to the perpendicular to the cutting edge (i.e. side W) by the chip flow angle η_c. Similarly, when modelling the shear plane heat source, the angular deviation η_s of the shear velocity vector V_s from the perpendicular to the cutting edge must be taken into account. It follows that an analysis based on "obliquely moving" rectangular heat sources is required. The basic equations governing heat transfer across such obliquely moving heat sources have been derived recently [7]. These will now be summarised briefly.

Consider Fig. 1 which shows a rectangular heat source of dimensions $2l' \times 2m'$ moving on a semi-infinite conducting medium. The source velocity V relative to the medium has an obliquity Φ defined by the angular deviation of the velocity vector V from side $2l'$. Cartesian axes X and Y are parallel to these sides $2l'$ and $2m'$ respectively while the

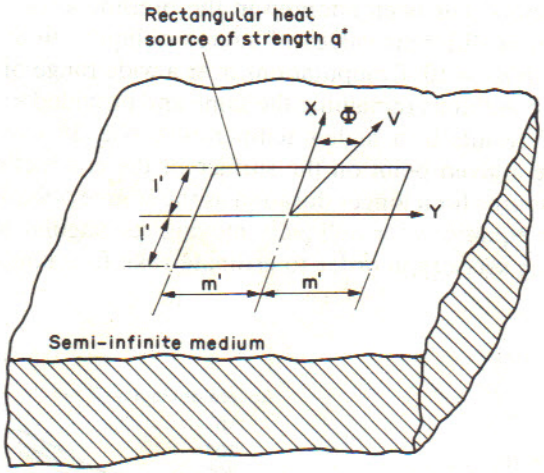

FIG. 1. A rectangular heat source moving obliquely on a semi-infinite conducting medium.

Z-axis is perpendicular to both X and Y. Let q^* be the uniformly distributed heat energy per unit area per unit time entering the conducting medium across the heat source. Let α_m and k_m be the thermal diffusivity and the thermal conductivity respectively of the conducting medium. Following (7), the temperature rise $\Delta\theta(x, y)$ at a point (x, y) on the conducting medium, in such a situation, can be expressed as:

$$\Delta\theta(x, y) = \frac{q^*\alpha_m}{k_m V (2\pi)^{\frac{1}{2}}} f_1 (X, Y, L, M, \Phi) \tag{1}$$

where the magnitude of the function $f_1 (X, Y, L, M, \Phi)$ is given by

$$f_1(X,Y,L,M, \Phi) = \int_0^\infty \left\{\text{erf}\left(\frac{X + L + w^2 \cos\Phi}{\sqrt{2}\, w}\right) - \text{erf}\left(\frac{X - L + w^2 \cos\Phi}{\sqrt{2}\, w}\right)\right\}$$
$$\left\{\text{erf}\left(\frac{Y + M + w^2 \sin\Phi}{\sqrt{2}\, w}\right) - \text{erf}\left(\frac{Y - M + w^2 \sin\Phi}{\sqrt{2}\, w}\right)\right\} dw \tag{2}$$

in which

$$X = \frac{Vx}{2\alpha_m},\ Y = \frac{V_y}{2\alpha_m},\ L = \frac{Vl'}{2\alpha_m},\ M = \frac{Vm'}{2\alpha_m},\ w = \left(\frac{V^2 t}{2\alpha_m}\right)^{\frac{1}{2}} \text{ and } t = \text{time}. \tag{3}$$

When $\Phi = 0$, these equations reduce to the equations of Carslaw and Jaeger [5] for orthogonally moving rectangular heat sources as, indeed, they should.

The mean temperatures rise $\Delta\bar{\theta}$ over the source area is obviously

$$\Delta\bar{\theta} = \frac{q^*\alpha_m \bar{f}_1}{k'_m V (2\pi)^{\frac{1}{2}}} \tag{4}$$

where

$$\bar{f}_1 = \frac{1}{4l'm'} \int_{-m'}^{m'} \int_{-l'}^{l'} f_1 (X, Y, L, M, \Phi)\, dx, dy. \tag{5}$$

No explicit expression is available for the estimation of the definite integral involved in equation (5) but it may be evaluated using the Gaussian quadrature technique. Such a

procedure, using 16 knots, has been adopted in the present work. Figure 2 shows the results of computation at different values of source obliquity Φ and non-dimensional source velocity L and $m'/l' = 10$. Computations over a wide range of values of Φ, L and m'/l' show that, other conditions remaining the same and provided $m'/l' > 1$, an increase in source obliquity Φ results in a higher temperature rise $\Delta\bar{\theta}$ over the source. Very simply, this is because a given point on the surface of the conducting medium stays in contact with the heat source for a longer duration as the source obliquity, Φ, is increased.

These heat transfer equations for obliquely moving rectangular heat sources will be applied in the following sections in order to estimate rake face temperatures in oblique cutting.

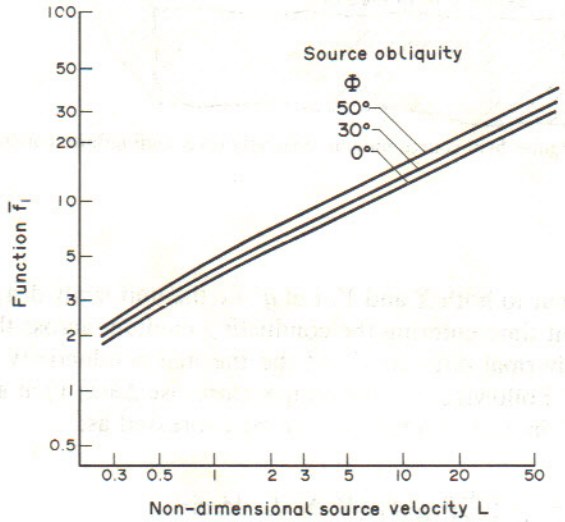

FIG. 2. Influence of source obliquity Φ and non-dimensional source velocity L on the mean temperature generated over an obliquely moving heat source (for aspect ratio, $m'/l' = 10$).

THEORETICAL ANALYSIS OF TEMPERATURES IN FREE OBLIQUE CUTTING

Basic assumptions

This analysis of free oblique cutting temperatures is based on the following assumptions:

1. The tool is ideally sharp and unworn;
2. The chip formation is continuous without a built up edge and the shear zone can be approximated as a shear plane;
3. The chip moves as a rigid body relative to the tool;
4. The heat flow is steady in the cutting tool and quasi-steady in the chip and the workpiece;
5. The rate of heat generation at the shear plane is uniformly distributed;
6. The rate of heat generation at the tool–chip interface is uniformly distributed over the sticking zone and decreases linearly over the sliding zone — becoming zero at the point where the chip leaves the rake surface;
7. The temperature of the chip as it leaves the shear zone is uniform;
8. Relative to the dimensions of the heat source at the tool–chip interface, the dimensions of the chip are sufficiently large to permit it to be viewed as a semi-infinite medium when modelling the moving heat source effect at the tool–chip interface. Likewise, the dimensions of the workpiece are sufficiently large to view it as a semi-infinite medium when modelling the moving heat source effect at the shear plane;

9. Relative to the dimensions of the tool–chip interface, the dimensions of the tool are sufficiently large to permit it to be viewed as a quarter-infinite medium when modelling the stationary heat source effect at the tool–chip interface;
10. Heat losses due to convection and radiation from all the surfaces of the workpiece, the chip and the tool may be ignored;
11. The chip thickness is the same in any section normal to the cutting edge; and
12. The directions of the shear force S on the shear plane and of the tangential force F on the rake surface are collinear with the directions of the velocity of shear V_s on the shear plane and the chip speed V_c respectively.

It may be noted that all of these assumptions, with the exception of assumption 6, are implicit in the analysis of Chao and Trigger [3] applicable to orthogonal cutting. Assumption 6 follows a refinement introduced by Wright *et al.* [4].

The mean shear plane temperature $\bar{\theta}_s$

The cutting parameters needed in order to estimate the mean shear plane temperature $\bar{\theta}_s$ are the dimensions of the shear plane, the normal shear angle Φ_n, the angular deviation η_s of the shear velocity vector V_s from the normal to the cutting edge in the shear plane, the shear velocity V_s and the mean heat generation rate per unit area q_s at the shear plane. These may be determined from experimental values of chip thickness ratio t_2/t_1 and reduced cutting forces (f_c, f_v and f_r) using the relationships [8, 9] summarised in the Appendix 1. The mean shear plane temperature $\bar{\theta}_s$ can now be calculated by following the procedure adopted by Loewen and Shaw for orthogonal cutting [2] but taking into account the obliquity of motion of the shear plane heat source.

Let R_s be the fraction of shear plane heat flux that leaves with the chip. The rise in temperature due to this heat flux is

$$\Delta\bar{\theta}_{s,\,c} = \frac{R_s q_s}{c_s V \sin\phi_n} \tag{6}$$

where c_s is the volume specific heat of the chip material, which may be estimated at temperature $(\theta_0 + \bar{\theta}_s)/2$, V is the cutting speed and ϕ_n is the normal shear angle.

Clearly, $(1 - R_s)q_s$ is the rate of heat per unit area entering the work material from the shear plane. From the point of view of the workpiece this source may be idealised as a heat source moving on the semi-infinite workpiece. The actual source is a parallelogram but, as an approximation, it will be taken as a rectangular source of dimensions W and t_1 cosec ϕ_n moving with velocity V_s at an obliquity η_s. Applying equation (4), the mean temperature rise on the shear plane from this moving heat source may be expressed as

$$\Delta\bar{\theta}_{s,\,w} = \frac{(1 - R_s)\, q_s \alpha_s \bar{f}_1}{k_s V_s (2\pi)^{\frac{1}{2}}} \tag{7}$$

where k_s and α_s are the thermal conductivity and diffusivity of the workpiece material at the temperature $\bar{\theta}_s$; and the magnitude of $\bar{f}_1$ is obtained from equation (5) using the substitutions (see equations (3)):

$$\Phi = \eta_s;\ V = V_s;\ L = \frac{V_s t_1 \text{ cosec } \phi_n}{4\alpha_s} \text{ and } M = \frac{V_s W}{4\alpha_s}. \tag{8}$$

Now from Blok's Partition Principle [10], $\Delta\bar{\theta}_{s,\,c}$ and $\Delta\bar{\theta}_{s,\,w}$ are merely two different expressions for the mean temperature rise at the shear plane, so that

$$\Delta\bar{\theta}_{s,\,c} = \Delta\bar{\theta}_{s,\,w}\,. \tag{9}$$

Combining equations (6), (7), (8) and (9) an expression for R_s may be obtained. The

mean temperature rise $\Delta\bar{\theta}_{s,c}$ (or $\Delta\bar{\theta}_{s,w}$) may be obtained by substituting this value of R_s in either equation (6) or (7). Finally the mean shear plane temperature is given by

$$\bar{\theta}_s = \theta_0 + \Delta\bar{\theta}_{s,c} = \theta_0 + \Delta\bar{\theta}_{s,w} \tag{10}$$

where θ_0 is the ambient temperature.

Source idealisation at the tool–chip contact area

Figure 3 illustrates the source idealisation at tool–chip contact area in free oblique cutting similar to that used by Chao and Trigger in their analysis of orthogonal cutting [3]. The tool–chip contact area is a parallelogram of base W and height C_n. This contact area may be viewed as a stationary heat source lying on the quarter-infinite conducting medium of the tool (ignoring the effect of non-zero rake and clearance angles). As an approximation, the heat source at the rake face is replaced by m contiguous rectangular band sources of width $2\Delta x$ (equal to C_n/m) with each band source being identified by index i.

Moving heat sources on chip side at the rake surface

At the rake surface, as viewed from the chip, there are m contiguous rectangular heat sources moving at a speed equal (but opposite in direction) to the chip velocity V_c. The source velocity V_c is inclined to the normal to the cutting edge by the chip flow angle η_c. i.e. the source obliquity is η_c. Following equation (1), the temperature rise at the centre of a rectangular sub-area i due to a uniform heat flux $q_{c,i'}$ per unit area per unit time entering the chip over source element i can be expressed as

$$\Delta\theta_{c,i'i} = q_{c,i} I(i',i) \tag{11}$$

where the influence coefficient $I(i', i)$ is given by

$$I(i', i) = \left\{\frac{\alpha_s}{k_c V_c (2\pi)^{\frac{1}{2}}}\right\} f_1 (X_{i'i}, Y_{i'i}, L_c, M_c, \eta_c) \tag{12}$$

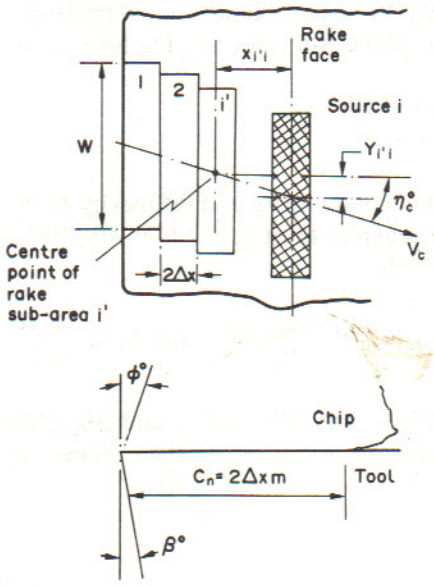

FIG. 3. Source idealisation at tool–chip contact area in oblique cutting for zero rake tool.

k_c and α_c being the thermal conductivity and thermal diffusivity of the chip material (at the rake temperature). The relevant form of the function f_1 in equation (12) is obtained by making the following substitutions in equation (1);

$$X = X_{i'i} = 2\Delta x(i - i')\, V_c/2\alpha_c,$$

$$Y = Y_{i'i} = X_{i'i} \tan \eta_c,\ L = L_c = V_c\, x/2\alpha_c,$$

$$M = M_c = V_c W/4\alpha_c \text{ and } \Phi = \eta_c. \tag{13}$$

The resultant temperature at the centre of sub-area i' due to the combined effect of the m contiguous moving rake sources is then

$$\theta_{c,\,i} = \bar{\theta}_s + \sum_{i=1}^{m} q_{c,\,i} I(i',\, i). \tag{14}$$

Stationary heat sources on tool side at the rake surface

From the point of view of the tool there are m stationary rectangular sources of variable intensity distributed over the rake surface. However, to facilitate the assumption of a semi-infinite medium, it is necessary to create m mirror images of these sources on the other side of the cutting edge. Thus, for every source i there is a mirror image $\bar{i}$. Figure 4 shows the resulting situation at the rake surface. The temperature rise at sub-area i' due to a uniform heat flux $q_{t,\,i}$ per unit area per unit time entering the tool over the source i is

$$\Delta\theta_{t',\,i'i} = q_{t,\,i}\, J'(i',\, i) \tag{15}$$

where

$$J'(i',i) = \frac{2}{2\pi k_t} \int_{-W/2}^{W/2} dy' \int_{-\Delta x}^{\Delta x} \frac{dx'}{\{(X_t - x')^2 + (Y_t - y')^2\}^{\frac{1}{2}}} \tag{16}$$

$$X_t = 2\Delta x\ (i' - i) \tag{17}$$

$$Y_t = 2\Delta x\ (i' - i) \tan \eta_c \tag{18}$$

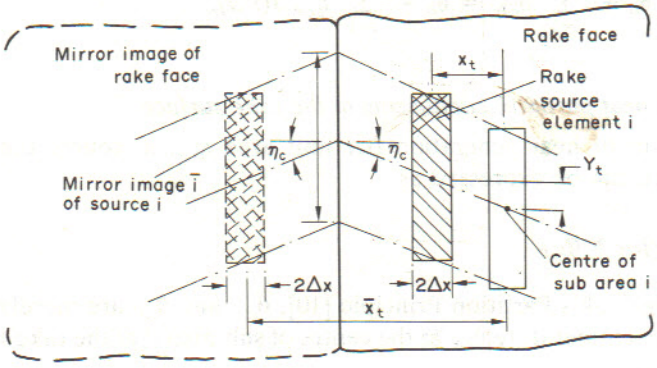

FIG. 4. Mirror images $\bar{i}$ corresponding to each rake source element i.

and k_t is the thermal conductivity of the tool material at the prevailing temperature.

On integration equation (16) gives

$$J'(i', i) = f_2(X_t, Y_t, \Delta x) \tag{19}$$

where (following [3])

$$f_2(X_t, Y_t, \Delta x) = \frac{1}{2\pi k_t}\{|X_t + x|\left(\sinh^{-1}\frac{Y_t + W/2}{X_t + \Delta x} - \sinh^{-1}\frac{Y_t - W/2}{X_t + \Delta x}\right)$$

$$+ |X_t - x|\left(\sinh^{-1}\frac{Y_t - W/2}{X_t - \Delta x} - \sinh^{-1}\frac{Y_t + W/2}{X_t - \Delta x}\right)$$

$$+ |Y_t + W/2|\left(\sinh^{-1}\frac{X_t + \Delta x}{Y_t + W/2} - \sinh^{-1}\frac{X_t - \Delta x}{Y_t + W/2}\right)$$

$$+ |Y_t - W/2|\left(\sinh^{-1}\frac{X_t - \Delta x}{Y_t - W/2} - \sinh^{-1}\frac{X_t + \Delta x}{Y_t - W/2}\right)\}. \tag{20}$$

The effect of mirror images is similarly obtained by writing

$$\Delta\theta_{t'i\bar{i}} = q_{t,\bar{i}}\ J''(i', \bar{i}) \tag{21}$$

where

$$q_{t,\bar{i}} = q_{t,i} \tag{22}$$

and $J''(i',i)$ is equal to function $f_2(\bar{X}_t, \bar{Y}_t, \Delta x)$ obtained by substituting $\bar{X}_t = 2\Delta x(i' + i - 1)$ for X_t in equation (19).

The temperature rise at the centre of sub-area i' due to the combined effect of source i and its mirror image $\bar{i}$ is

$$\Delta\theta_{t,i'i} = \Delta\theta'_{t,i'i} + \Delta\theta''_{t,i'\bar{i}} = q_{t,i}J(i',i) \tag{23}$$

where

$$J(i',i) = J'(i', i) + J''(i', \bar{i}). \tag{24}$$

The resultant temperature at sub-area i' due to the combined effect of the m contiguous stationary rectangular heat sources at the tool–chip interface is then given by

$$\theta_{t,i'} = \theta_0 + \sum_{i=1}^{m}\theta_{t,ii'} = \theta_0 + \sum_{i=1}^{m} q_{t,i'}\,J(i',i). \tag{25}$$

Temperature and heat partition coefficients at the rake surface

Clearly, the rate of heat generation per unit area $q_{r,i}$, at source element i at the tool–chip interface can be expressed as

$$q_{r,i} = q_{c,i} + q_{t,i}. \tag{26}$$

Further, following Blok's Partition Principle [10], $\theta_{c,i'}$ and $\theta_{t,i'}$ are merely two different expressions for the temperature $\theta_{r,i'}$ at the centre of sub-area i' at the rake surface so that

$$\theta_{c,i'} = \theta_{t,i'} = \theta_{r,i'}. \tag{27}$$

Combining equations (14), (25), (26) and (27), it is possible now to determine the temperature distribution $\theta_{r,i'}$ at the rake surface as well as the magnitude of $q_{t,i}$ for any i from known values of θ_0 and $\bar{\theta}_s$, and a given distribution of heat generation $q_{r,i}$ at the rake surface.

The mean rake tool–chip interface temperature is then given by

$$\bar{\theta}_r = \frac{1}{m} \sum_{i'=1}^{m} \theta_{r,i'}. \tag{28}$$

The heat partition coefficient, expressed as the fraction entering the tool, at source element i is

$$R_{r,i} = q_{t,i} / q_{r,i} \tag{29}$$

so that the mean partition coefficient of heat at the tool–chip interface is

$$\bar{R}_r = \frac{1}{m} \sum_{i=1}^{m} R_{r,i}. \tag{30}$$

Equation (28) will be used later to compute $\bar{\theta}_r$ from experimental data on chip thickness, chip flow angle, tool–chip contact length and cutting forces obtained while machining mild steel with H.S.S. tools. The validity of the computed variations of $\bar{\theta}_r$ will then be examined in the light of empirical evidence on tool–work thermocouple temperature, θ_m.

EXPERIMENTAL DETAILS

Cutting tests were performed on a Colchester Triumph 2000 lathe using MTM 41 H.S.S. (RC65) cutting tool bits with 10° normal rake angle, 5° normal clearance angle and obliquities in the range 0–50°. Tubular mild steel workpieces (OD 50.8 mm, wall thickness 2 mm and BHN 120) were cut at different speeds (25–55 m/min) and feeds (0.05–0.2 mm/rev). The speed range selected was sufficiently high to avoid the occurance of built up edge. All tools used were sharp and no cutting fluid was used.

Cutting forces F_c, F_v and F_r were measured using a Kistler three-component measuring platform the outputs from which were fed to a UV recorder. Cutting temperatures were measured by the tool–work thermocouple method. The tools were 150 mm long and leads to a digital voltmeter were connected to the far ends of the tools which were cooled by an air jet so as to minimise errors due to parasitic emfs. For each tool, the calibration of the tool–work thermocouple was effected by using the silver bead technique. The resulting calibration curves were similar to those reported in [11]. Chip flow angles were estimated by the technique described in [12]. Shallow axial slots were machined on the workpieces so that chip lengths corresponding to one revolution of the workpiece could be obtained. The chip thickness ratios were estimated from the measured values of chip flow angle and chip length ratio. Tool–chip contact lengths were estimated by viewing the scratch patterns left by the sliding chips on the rake surface of freshly ground tools.

RESULTS AND DISCUSSION

Figure 5 shows the measured dependence of t_2/t_1, C_n and η_c on tool obliquity λ when V = 41 m/min and t_1 = 0.1 mm while Fig. 6 shows the relation between cutting force components F_c, F_v and F_r and tool obliquity λ at the same cutting conditions. These results are similar to those reported in earlier works an oblique cutting [8, 9, 12]. Tests at other cutting speeds in the range 22 to 55 m/min, indicated that changing the cutting speed does not produce significant changes in the above variations. In the cutting speed range 55 to 74 m/min slight decreases in t_2/t_1 and C_n were obtained. Tests at other values of t_1, in the range 0.05 to 0.2 mm, showed that F_c, F_v, F_r and C_n varied linearly with t_1 whereas t_2/t_1 and η_c were independent of changes in t_1.

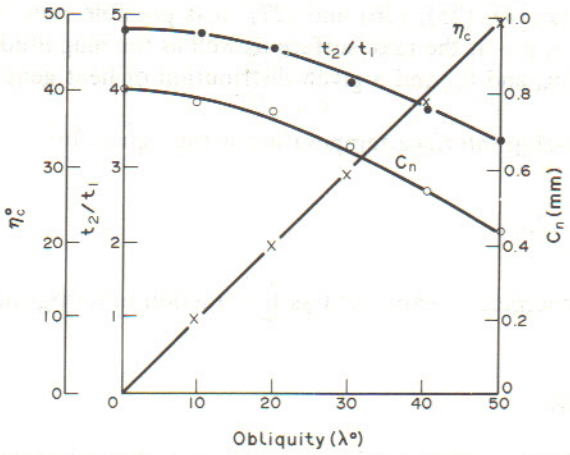

FIG. 5. Empirical variation of $t_2/t_1/C_n$ and η_c with tool obliquity (mild steel work piece, H.S.S. tool, dry cutting, $\alpha_n = 10°$, $\beta_n = 5°$, $b = 2$ mm, $V = 41$ m/min, and $t_1 = 0.1$ mm).

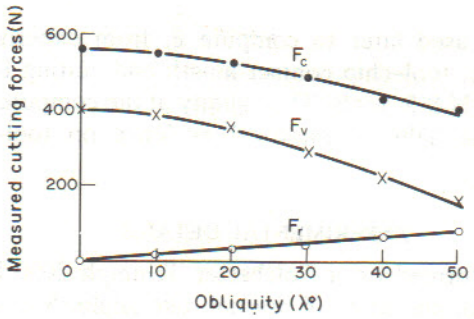

FIG. 6. Measured variation of cutting force components F_c, F_v and F_r with tool obliquity (cutting conditions as in Fig. 5).

These experimental data were processed by using a computer programme based on the temperature analysis for free oblique cutting developed earlier and the equations are presented in the Appendix. The computer programme utilised the thermal properties for mild steel quoted in [2] and an iteration procedure was adopted to allow for the temperature dependence of the workpiece properties. Due to lack of precise information, the H.S.S. tool thermal conductivity was taken to be equal to that of the workpiece. Values of $m = 7$ and $m'' = 5$ were assumed.

Figures 7 and 8 show the computed distributions of temperature θ_r and heat partition coefficient R_r at the tool–chip interface when $V = 41$ m/min and $t = 0.1$ mm for $\lambda = 0$ and 50°. It is clear that, in this range, tool obliquity has no significant effect on the form of these distributions. Further, these distributions exhibit the same characteristics as those obtained by Chao and Trigger [3] for orthogonal cutting with carbide tools.

Figures 9 and 10 show the computed variations of the mean shear plane temperature, $\bar{\theta}_s$, (depicted by broken lines) and of the mean tool–chip interface temperature, $\bar{\theta}_r$, at the rake face (depicted by continuous lines) with cutting speed, V, and uncut chip thickness, t_1, respectively when $\lambda = 0$ and 50°. It is seen that both $\bar{\theta}_s$ and $\bar{\theta}_r$ can be expressed by power laws of the form

$$\bar{\theta}_r = K_s V^{\epsilon'} t_1^{\eta'} \text{ and } \bar{\theta}_r = K_r V^{\epsilon_r} t_1^{\eta_r} \tag{31}$$

where constants K_s and K_r decrease with increasing λ and the indices ϵ', η', ϵ_r and η_r show some dependence on λ as evidenced by their magnitudes listed for $\lambda = 0$ and 50° in Figs 9 and 10.

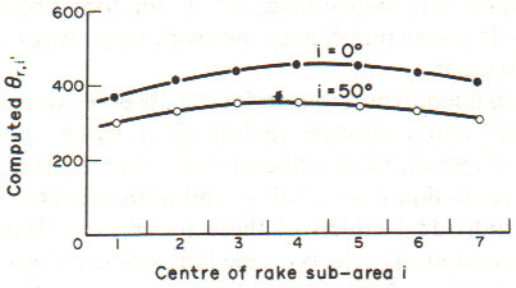

FIG. 7. Computed temperature distributions, θ_r, at the rake face for $\lambda = 0$ and 50° (cutting conditions as in Fig. 5).

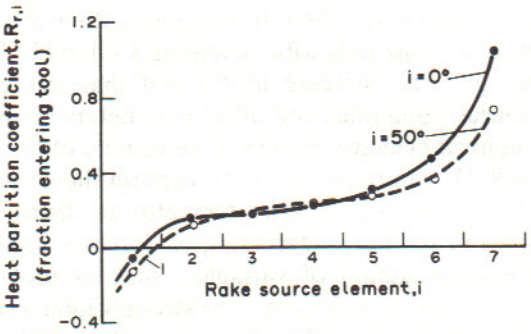

FIG. 8. Computed distributions of heat partition coefficient, R_r, at the rake face for $\lambda = 0$ and 50° (cutting conditions as in Fig. 5).

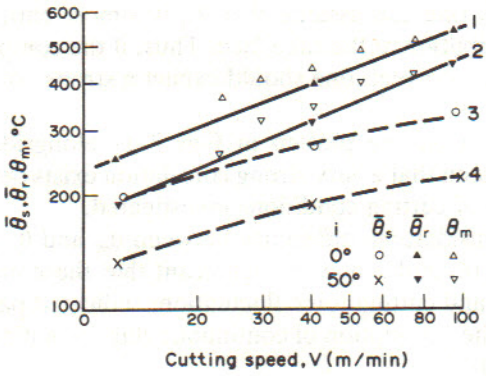

FIG. 9. Computed variations of $\bar{\theta}_s$ and $\bar{\theta}_r$ with cutting speed for $i = 0$ and $i = 50°$ (other conditions as in Fig. 5). 1. $\bar{\theta}_r$ at $i = 0°$; slope, $\epsilon_r = 0.4$; 2. $\bar{\theta}_r$ at $i = 50°$; slope, $\epsilon_r = 0.43$; 3. $\bar{\theta}_s$ at $i = 0°$; slope, $\epsilon_s = 0.26$; 4. $\bar{\theta}_s$ $i = 50°$; slope, $\epsilon_s = 0.25$. Also shown for comparison, empirical values of θ_m at $i = 0$ and $i = 50°$.

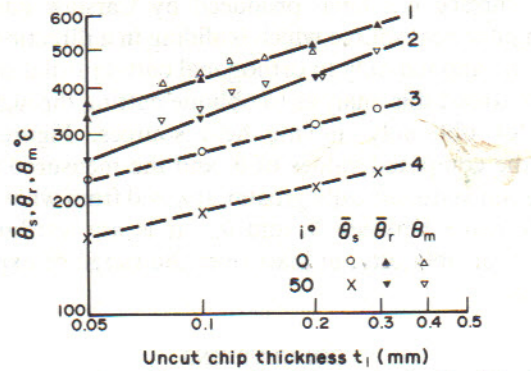

FIG. 10. Computed variations of $\bar{\theta}_s$ and $\bar{\theta}_r$ with un-cut chip thickness for $i = 0$ and $i = 50°$, (other conditions as in Fig. 5). 1. $\bar{\theta}_r$ at $i = 0°$; slope, $\eta_r = 0.35$; 2. $\bar{\theta}_r$ at $i = 50°$; slope, $\eta_r = 0.4$; 3. $\bar{\theta}_s$ at $i = 0°$; slope, $\eta_s = 0.27$; 4. $\bar{\theta}_s$ at $i = 50°$; slope, $\eta_s = 0.24$. Also shown, for comparison, empirical values of θ_m, at $i = 0$ and $i = 50°$.

Figures 11a and b show the dependence of $\bar{\theta}_r$ on tool obliquity λ at different combinations of V and t_1. It is seen that $\bar{\theta}_r$ decreases with increasing λ in the entire range of cutting conditions investigated.

It is difficult to quote an unequivocal reason for the observed decrease in the computed $\bar{\theta}_r$ with increasing λ since the temperature analysis given earlier indicates that there are several parameters through which λ can influence $\bar{\theta}_r$ viz. source strengths q_s and q_r; source velocities V_s and V_c; source obliquities η_s and η_c; and source lengths $t_1/\sin\Phi_n$ and C_n. It is not easy to isolate the individual effects of these parameters. Further, some of these parameters have mutually opposing effects on the temperature parameters. For instance, the heat dissipated in cutting tends to decrease as λ is increased. This results from the empirically observed decrease in cutting force F_c with increasing λ (see Fig. 6) so that $\bar{\theta}_r$ should tend to decrease. On the other hand, an increase in λ tends to increase the source obliquities (η_s and η_r) at the shear and rake planes which (as implied by Fig. 2) should result in an increase in $\bar{\theta}_r$. However, despite the above difficulties, sensitivity studies indicate that the observed decrease in $\bar{\theta}_r$ with increasing λ is largely due to the decrease in the specific cutting energy (i.e. decrease in F_c) and that this effect outweighs the influence of λ on the source obliquities and other parameters involved.

Consider now the empirical evidence by which the validity of the computed variations of $\bar{\theta}_r$ (illustrated in Figs 9–11) can be assessed. To confirm these variations, one can use either a direct procedure of measuring rake temperature distributions, say, through embedded thermocouples (a tedious undertaking of dubioius accuracy) or an indirect approach based on the investigation of variables, such as tool–work thermocouple temperature or crater wear, which are known to be strongly influenced by $\bar{\theta}_r$. Due to lack of information concerning crater wear of H.S.S. tools, we have little choice but to use the measured tool–work thermocouple temperature, θ_m, to check the validity of the computational procedures used for $\bar{\theta}_r$. Since only sharp cutting tools have been used in the present investigation, one can assume that θ_m is almost entirely the result of the contact temperature distribution at the rake face. Thus, if the computational procedures for $\bar{\theta}_r$ as a function of λ are correct, one should expect a strong correlation (though not identity) between θ_m and $\bar{\theta}_r$.

The measured values of θ_m are plotted in Figs 9–11 alongside the corresponding computed $\bar{\theta}_r$ curves. It is seen that a very strong correlation exists between θ_m and $\bar{\theta}_r$ over virtually the entire range of cutting conditions investigated.

(There is, however, considerable difference between θ_m and $\bar{\theta}_r$ when $V = 22$ m/min and $i = 0$ to 20° in Fig. 11a, and it may be significant that these are just the conditions when the observed chips and cutting force fluctuations indicated partially-discontinuous chip formation, i.e. that the assumption of continuous chip formation made in the theory leading to $\bar{\theta}r$ is violated.)

We might pause here to make clear exactly what we are trying to demonstrate and the extent to which we can be said to have succeeded. A long established analysis for the temperature generated at the interface between one smooth surface sliding on a semi-infinite smooth surface has been produced by Carslaw and Jaeger [5]. This is applicable to a rectangular heat source which is sliding in a direction parallel to one of its sides and, hence, can be applied only to orthogonal cutting situations [2, 3]. The present work is an attempt to extend this analysis to oblique cutting through the application of a recent solution [7] for obliquely moving heat sources. Figure 11 shows that the differences between the computed values of θ_r and the measured values of θ_m at given cutting conditions are not systematically greater at $\lambda \neq 0$ from what they are at $\lambda = 0$, i.e. whatever discrepancy exists between θ_r and θ_m, it is *not* attributable to the method adopted here to allow for obliquity, at least over the range of experimental conditions examined in this work.

CONCLUSIONS

The method proposed here for calculating rake temperatures in oblique cutting has been shown to account for the influence of obliquity to the same degree of accuracy as

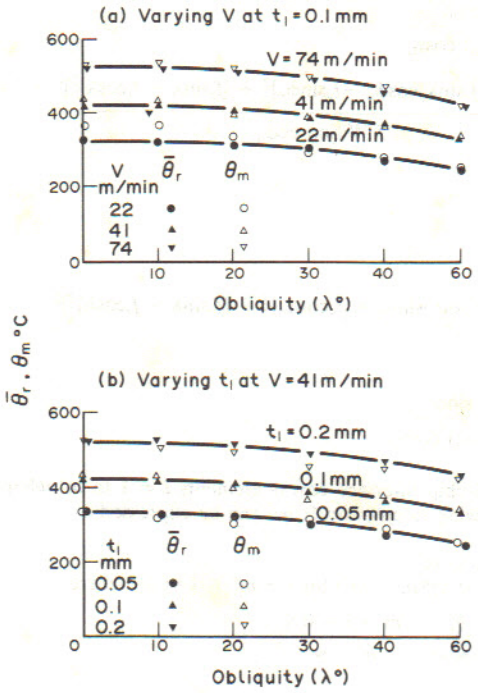

FIG. 11. Variation of $\bar{\theta}_r$ and θ_m with λ at various combinations of cutting speed and uncut chip thickness.

that obtained for orthogonal cutting (i.e. zero obliquity). This shows that the errors in the analysis arise from sources other than those elements introduced to reflect the influence of obliquity on temperature generation.

REFERENCES

[1] B. T. CHAO and K. J. TRIGGER, *Trans. Am. Soc. Mech. Engrs* **77**, 1107 (1955).
[2] E. G. LOEWEN and M. C. SHAW, *Trans. Am. Soc. Mech. Engrs* **76**, 217 (1954).
[3] B. T. CHAO and K. J. TRIGGER, *Trans. Am. Soc. Mech. Engrs* **80**, 311 (1958).
[4] P. K. WRIGHT, S. P. MCCORMICK and T. R. MILLER, *J. Engng Ind. Ser. B* **102**, 123 (1980).
[5] H. S. CARSLAW and J. C. JAEGER, *Introduction to the Mathematical Theory of Conduction of Heat in Solids*, 2nd Edn., The Clarendon Press, Oxford (1959).
[6] J. C. JAEGER, *Proc. R. Soc. N.S.W.* **76**, 203 (1942).
[7] V. V. S. SASTRY, T. L. SITHARAMA RAO and P. K. VENUVINOD, 6th National Heat and Mass Transfer Conference, Indian Institute of Technology, Madras, E-39 (1981).
[8] M. C. SHAW, N. H. COOK and P. A. SMITH, *Trans. Am. Soc. Mech. Engrs* **74**, 1055 (1952).
[9] N. N. ZOREV, *Metal Cutting Mechanics*, 1st Edn. Pergamon Press, Oxford (1966).
[10] H. BLOK, *Proc. General Discussion on Lubrication and Lubricants*, p. 222, Inst. Mech. Engrs, London (1938).
[11] W. S. LAU, P. K. VENUVINOD and G. RUBENSTEIN, *Int. J. Mach. Tool Des. Res.* **20**, 29 (1980).
[12] P. K. VENUVINOD and W. S. LAU, *Microtecnic* **2**, 32 (1977).

APPENDIX

THE FOLLOWING relationships can be easily obtained from well known analyses [8, 9] of oblique cutting.

$$\eta_s = \arctan\left(\tan\lambda\cos(\phi_n - \alpha_n) - \tan\eta_c\sin\phi_n\right)/\cos\alpha_n \tag{A.1}$$

where

$$\phi_n = \arctan\frac{\cos\alpha_n}{\frac{t_2}{t_1} - \sin\alpha_n} \tag{A.2}$$

$$V_s = \frac{V\cos\alpha_n\cos\lambda}{\cos(\phi_n - \alpha_n)\cos\eta_s} \tag{A.3}$$

$$q_s = \frac{[\{(f_c\cos\lambda + f_r\sin\lambda)\cos\phi_n - f_v\sin\phi_n\}^2 + \{f_c\sin\lambda - f_r\cos\lambda\}^2]^{\frac{1}{2}}}{J\,W\,t_1\operatorname{cosec}\phi_n} \tag{A.4}$$

$$q_r = \frac{R\,V_c}{W\,C_n\,J} \tag{A.5}$$

where

$$F = [\{(f_c\cos\lambda + f_r\sin\lambda)\sin\alpha_n + f_v\cos\alpha_n\}^2 + (f_c\sin\lambda - f_r\cos\lambda)^2]^{\frac{1}{2}} \tag{A.6}$$

and

$$V_c = \frac{V\cos\lambda\sin\phi_n}{\cos(\phi_n - \alpha_n)\cos\eta_c}. \tag{A.7}$$

The sticking zone at the tool–chip interface covers elements $i = 1$ to m'' whereas the sliding zone cover sources $i = m'' + 1$ to m. Following assumption 6, $q_{r,i}$ can be expressed as

$$\begin{aligned} q_{r,i} &= u \text{ for } i = 1 \text{ to } m'' \\ &= u(m - i + 0.5)/(m - m'') \text{ for } i = m'' + 1 \text{ to } m, \text{ where} \end{aligned} \tag{A.8}$$

$$u = mq_r/\{m'' + \sum_{j=m''+1}^{m} \frac{m - j + 0.5}{m - m''}\}. \tag{A.9}$$